Hygrothermal effects on fatigue delamination behavior in composite laminates

Yao, Liaojun; Wang, Jiexiong; He, Yonglyu; Zhao, Xiuhui; Chen, Xiangming; Liu, Jurui; Guo, Licheng; Alderliesten, R. C.

DOI
10.1016/j.compstruct.2023.117830

Publication date
2024

Document Version
Final published version

Published in
Composite Structures

Citation (APA)
Yao, L., Wang, J., He, Y., Zhao, X., Chen, X., Liu, J., Guo, L., & Alderliesten, R. C. (2024). Hygrothermal effects on fatigue delamination behavior in composite laminates. *Composite Structures*, *330*, Article 117830. https://doi.org/10.1016/j.compstruct.2023.117830

Composite Structures 330 (2024) 117830

Contents lists available at ScienceDirect

Composite Structures

journal homepage: www.elsevier.com/locate/compstruct

Hygrothermal effects on fatigue delamination behavior in composite laminates

Liaojun Yao [a,*], Jiexiong Wang [a], Yonglyu He [b,*], Xiuhui Zhao [b], Xiangming Chen [c], Jurui Liu [a], Licheng Guo [a], R.C. Alderliesten [d]

[a] *Department of Astronautics Science and Mechanics, Harbin Institute of Technology, Harbin, PR China*
[b] *Department of Material Science and Engineering, National University of Defense Technology, Changsha, PR China*
[c] *National Key Laboratory of Strength and Structural Integrity, AVIC Aircraft Strength Research Institute of China, Xi'an, PR China*
[d] *Structural Integrity and Composite Group, Faculty of Aerospace Engineering, Delft, the Netherlands*

ARTICLE INFO

Keywords:
Fatigue
Delamination
Hygrothermal aging
Composite laminates

ABSTRACT

Fatigue delamination growth (FDG) is an important failure in composite structures during their long-term operations. Hygrothermal aging can have significant effects on interlaminar resistance. It is therefore really necessary to explore FDG behavior in composite laminates with hygrothermal aging. Dynamic mechanical thermal analysis (DMTA), mode I FDG experiments and fractographic examinations were conducted to fully investigate hygrothermal aging effects and the corresponding mechanisms on FDG behavior. The DMTA results indicated that environmental aging can induce obvious T_g decrease. Mode I experimental fatigue data interpreted via different Paris-type correlations demonstrated that: Bridging has obvious retardation effects on FDG behavior via the Paris interpretations; The modified Paris relation can well characterize the intrinsic FDG behavior around the crack front; The use of the two-parameter Paris-type relation can appropriately account for *R*-ratio effects, contributing to a master resistance curve in determining mode I FDG behavior. According to these interpretations, it can be concluded that hygrothermal aging can have adverse effects on mode I FDG behavior. SEM examinations demonstrated that moisture absorption can cause fibre/matrix debonding and resin matrix pores/voids in the composite. However, no obvious difference in damage mechanisms was identified in mode I fatigue delamination for composite with/without environmental conditioning. Both fibre/matrix debonding and matrix brittle fracture were identified on fatigue fracture surfaces. Accordingly, it was concluded that fibre/matrix interface and matrix degradation induced by water absorption were the main reasons for a faster mode I fatigue crack growth in environmental aged composite.

1. Introduction

Carbon fibre reinforced polymer composites have been increasingly used in aerospace industry, for their excellent specific mechanical properties, weight saving potential, design and production flexibility, as compared to the traditional metallic materials. The use of these materials have been updated from secondary to primary structures, contributing to the weight percentage up to 50–52 % in the modern commercial aircrafts Boeing 787 and Airbus A350XWB [1]. Even though these materials take advantage of excellent in-plane mechanical performance, they are vulnerable to FDG, a unique damage evolution frequently reported between neighbored layers [2–4]. The initiation and propagation of this damage can gradually cause strength/stiffness degradation, and may finally result in catastrophic failure of a composite structure during its service life. Incorporating with an important change of the composite structure certification philosophy from *no crack growth* to *slow crack growth* recommended by the US federal aviation administration since 2009 [5], it is therefore crucial to explore FDG behavior of composite materials in order to guarantee the integrity of composite structures in their long-term operations. As a result, both the European Structural Integrity Society Technical Committee 4 (ESIS TC4) and the American Society for Testing and Materials, International, Subcommittee D30.06 (ASTM D30.06) have performed separate round-robin test programs in the last decade for the purpose of developing a test standard for mode I FDG in composites [6–8].

Researchers [1–4,9–15] indeed have conducted a large number of

* Corresponding authors.
E-mail addresses: L.Yao@hit.edu.cn (L. Yao), Yonglyu.He@foxmail.com (Y. He).

https://doi.org/10.1016/j.compstruct.2023.117830
Received 31 August 2023; Received in revised form 22 November 2023; Accepted 17 December 2023
Available online 20 December 2023

experimental and numerical studies to determine FDG behavior in composite laminates at ambient conditions in the past several decades. However, it must be stressed that composite structures can endure unavoidable hygrothermal conditions during their long-term operations. And it has been reported that environmental conditions can have important effects on the performance of composite materials [2]. Particularly, aging by water absorption, i.e. hygrothermal aging, can have significantly detrimental influence on composites' mechanical performance [16–18], making it crucial to have thorough investigations on the durability of these materials with hygrothermal exposure. And there is sufficient evidence that humidity degradation of composite materials can cause significant accidents of an aircraft in its long-term usage [19].

There are three main mechanisms for moisture uptake in carbon fibre reinforced epoxy composite laminates [17,19,20]: water absorption in polymer matrix; water diffusion at fibre/matrix interface because of capillary/wicking effects; and water uptake via microscopic voids. In addition, it is worth noting that epoxy resin is a hydrophilic material with natural capacity of water absorption [19], promoting moisture absorption in carbon fibre reinforced epoxy composites. It has been generally reported in literatures [20–24] that moisture diffusion in composite materials can not only cause matrix plasticization/degradation, but also lead to significant fibre/matrix interface debonding. In addition, hygrothermal-induced swelling can result in internal stress at the interphase region, i.e. around fibre/matrix interface, which can also reduce the adhesion integrity between reinforced fibre and epoxy matrix [20,25,26]. All these changes in resin matrix and around fibre/matrix interface are intuitively expected to have important effects on interlaminar resistance of a composite material, as it significantly depends on the properties of matrix and fibre/matrix interface. As a result, it is necessary to have thorough investigations on FDG behavior not only in ambient conditions, but also in unavoidable hygrothermal environments.

Researchers [23,27–33] indeed have paid a lot of attention to hygrothermal aging effects on interlaminar strength and quasi-static delamination resistance. People have made a consensus that [23,27–30] there is obvious reduction in interlaminar shear strength of composite materials after water absorption. The major reason for this reduction attributes to hygrothermal-induced fibre/matrix interface degradation. However, there is no consensus on hygrothermal aging effects on quasi-static delamination behavior. Alessi et al [20] reported that no obvious deviation on mode I fracture toughness after hygrothermal conditioning. Particularly, it was concluded that this unaltered behavior might be related to a balance of prevailing toughening or embrittling mechanisms activated by the aging conditions. Davidson et al [24] investigated hygrothermal aging effects on delamination resistance at different mode ratios. It was found that interlaminar resistance can increase in mode I delamination, but decrease in mode II. The reason for mode I resistance increase is related to the increase of matrix ductility. However, less amount of damage evolution can be generated on mode II fracture surface after moisture absorption, finally contributing to resistance decrease. And for mixed-mode I/II delamination, fracture toughness demonstrated a blend of pure mode behaviors. In another experimental study conducted by Asp [31], it was reported that hygrothermal aging has negligible effect on mode I initial delamination resistance, but leads to reduction in interlaminar resistance of both mode II and mixed-mode I/II. Mamalis et al [32] investigated the effects of seawater aging on mode I delamination behavior of three different types of unidirectional composite laminates. It was found that hygrothermal treatment can cause obvious reduction in the initiation delamination resistance of all these composites, because of weakening fibre/matrix interface. Scholars [33] conducted experimental study on hygrothermal aging effects on mixed-mode I/II delamination resistance of composite joints with different bonded technologies (i.e. co-cured (CC) without adhesive, co-bonded (CB) and secondary bonded (SB)). The results indicated that composite joint with SB bonded technology demonstrates better delamination resistance as compared to joints with the other two bonded technologies.

To the best knowledge of the authors, only a limited number of studies have been conducted in the past to determine FDG behavior in composites after hygrothermal aging. And there is no consensus on hygrothermal aging effects on FDG behavior. Nakai et al [34] conducted fatigue delamination experiments on two kinds of composites (i.e. T300/3601 and M40J/2500) with/without water absorption. It was found that water uptake can decrease Mode I FDG of both materials, for the increase of ductility in the resin matrix. However, in a study provided by Landry et al [35], it was reported that moisture absorption can have adverse influence on mode I FDG behavior, i.e. environmental conditioning can accelerate FDG. Similar conclusion was also made by the same authors in mode II FDG [36]. Recently, researchers [37] provided a comparison study on mode I and mode II onset fatigue delamination behavior of interlayer toughened composite joints with different bonded technologies. The results clearly demonstrated that the effects of hygrothermal aging on fatigue onset behavior are significantly dependent on bonded technologies. In another study [38], it was reported that hygrothermal aging can cause decrease of fatigue delamination in adhesively bonded composite structures, because of ductility increase in the bond.

According to above discussions, even researchers have got a consensus that hygrothermal aging can have detrimental effects on composite material performance, limited studies were conducted to determine delamination behavior of composite laminates with hygrothermal aging under fatigue loading, as well as to examine the corresponding physical mechanisms. And no consensus has been achieved for hygrothermal aging effects on FDG behavior in composite laminates until now. As a result, further investigations on FDG behavior of composite laminates are still required in this field. To this aim, DMTA experiments were carried out to determine hygrothermal effects on the dynamic mechanical response of the composite. Mode I FDG experiments were subsequently conducted on pre-conditioned composite specimens at different *R*-ratios to thoroughly determine hygrothermal aging effects on fatigue delamination behavior. SEM examinations were finally performed on both material morphology and delamination fracture surfaces to thoroughly investigate the physical reasons and damage mechanisms for hygrothermal aging effects on FDG behavior.

2. Material and specimen pre-conditioning

The composite material used here is carbon fibre/epoxy prepreg M30SC/DT120 (high strength and modulus carbon fibre/toughened thermosetting epoxy). Composite laminates were laid in the designed stacking sequence $[0_{16}//0_{16}]$ (// indicates the delamination plane). A Teflon insert film with 12.7 μm thickness was placed in the middle plane to introduce an initial delamination, typically around $a_0 = 60$ mm. Laminates were cured in the autoclave at a pressure of 6 bars and curing temperature of 120 °C for 90 min. After curing, composite laminates were C-scanned for imperfections. Samples were taken from these areas where no imperfections were identified via the non-destructive testing.

Double cantilever beam (DCB) specimens, $L = 200$ mm length by $B = 25$ mm width with thickness of $h = 5$ mm, were cut from composite laminates with a diamond-coated cutting machine. One side of each DCB specimen was coated with a thin layer of typewriter correction fluid to enhance the visibility of delamination front during fatigue tests. A strip of grid paper was pasted on the coated side of the sample to aid in measuring fatigue crack propagation length a-a_0.

DCB specimens were exposed to the required environmental condition at temperature 70 °C and relative humidity (RH) 85 %, using the WEISS WK111-340 environmental chamber, according to the ASTM D5229 standard [39]. The weights of three conditioned samples were measured with pre-defined time intervals until the moisture absorption equilibrium, i.e. in a state that the effective moisture equilibrium changes less than 0.02 % within the reference time span. These DCB

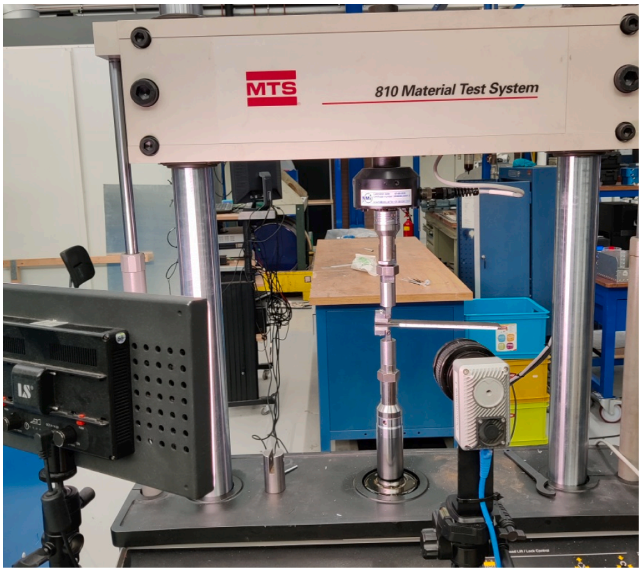

Fig. 1. Fatigue delamination experimental setup.

specimens with moisture saturation were well stored in the environmental chamber until the moment of their fatigue delamination experiments.

In accordance with the ASTM D5229 standard, the average moisture content M can be calculated with the measured mass information at different time intervals as

$$M = \frac{W_i - W_0}{W_0} \times 100 \tag{1}$$

where W_i is the current specimen mass; and W_0 is the initial specimen mass.

The single-phase Fickian diffusion model has been widely recommended and employed by different scholars [17,37] in determining the absorption curves of carbon fibre reinforced composite materials. Referring to the ASTM D5229 standard, the moisture diffusivity constant D_z can be determined as

$$D_z = \pi\left(\frac{h}{4M_m}\right)^2\left(\frac{M_2 - M_1}{\sqrt{t_2} - \sqrt{t_1}}\right)^2 \tag{2}$$

where h is the specimen thickness; M_m is the moisture equilibrium content; and $\left(\frac{M_2 - M_1}{\sqrt{t_2} - \sqrt{t_1}}\right)$ represents the slope of moisture absorption plot in the initial linear portion of the curve.

After the determination of the moisture diffusivity constant D_z, the moisture contents at different moments can be calculated with the following equation [32,39]

$$M_t = M_m\left\{1 - \frac{8}{\pi^2}\sum_{j=0}^{\infty}\frac{1}{(2j+1)^2}\exp\left[-\frac{D_z(2j+1)^2\pi^2 t}{h^2}\right]\right\} \tag{3}$$

3. Experimental procedure and data reduction methodology

3.1. Fatigue delamination experiments

All mode I fatigue experiments were conducted on a 15kN MTS servo-hydraulic test machine at a frequency of 5 Hz with stress ratios of $R = 0.1$ and 0.5 under displacement control. The load, displacement and number of cycles were automatically stored in an Excel file by the machine, enabling data reduction after the test. A computer controlled digital camera system with high resolution was employed to monitor delamination propagation via automatically recording an image of the tested specimen profile at pre-defined intervals. These recorded images could be subsequently analyzed to determine the fatigue delamination propagation length a-a_0. Detailed information of the experimental setup is demonstrated in Fig. 1.

Table 1
Mode I fatigue delamination test matrix.

Sample	R-ratio	Fatigue pre-crack propagation a-a_0 [mm]
85 %RH-1-R01	$R = 0.1$	4.60; 24.50; 43.15; 65.03; 91.02
85 %RH-2-R01		5.44; 22.01; 35.75; 50.06; 66.35; 77.41
85 %RH-1-R05	$R = 0.5$	4.09; 14.38; 26.37; 37.68; 50.20
85 %RH-2-R05		2.16; 8.80; 17.57; 24.96; 33.62; 42.88; 58.54; 71.24

Significant fibre bridging was observed in mode I fatigue delamination experiments in the previous studies [40,41]. To determine FDG behavior with different amounts of fibre bridging, DCB specimens were repeatedly tested for several times with increased displacements keeping the R-ratio constant. This specific test procedure has been introduced and used several times in fibre-bridged FDG characterization [40,41]. Particularly, FDG can gradually decrease with crack propagation in a displacement controlled fatigue test. This test was therefore manually terminated in case of crack retardation. After this, a monotonic loading–unloading cycle was conducted on this tested specimen to evaluate the minimum/maximum displacements which should be applied in the subsequent fatigue sequence. With this specific test procedure, multiple delamination resistance curves can be obtained, with each one representing delamination resistance equivalent to a specific fatigue pre-crack, i.e. delamination length at which that particular fatigue test was initiated. In addition, according to the monotonic loading–unloading cycle, interlaminar resistance at different fatigue crack lengths can be calculated to form the fatigue resistance curve (i.e. fatigue R-curve) $G_{IC}(a$-$a_0)$.

Table 1 provides a summary of all mode I FDG experiments with different fatigue pre-crack propagation (i.e. equivalent to different amounts of bridging fibres) at different stress ratios on DCB specimens with environmental conditioning. A total number of 24 fatigue experiments were conducted in the present study to explore mode I FDG behavior with hygrothermal aging.

3.2. Fatigue data reduction

The Modified Compliance Calibration (MCC) method Eq.(4), recommended in the ASTM D5528 standard, was employed to calculate the *SERR* G with the load, displacement and crack length information recorded in fatigue delamination tests. The 7-point Incremental Polynomial Method, recommended in the ASTM E647 standard, was used to fatigue crack growth rate da/dN calculation.

$$G = \frac{3P^2C^{(2/3)}}{2A_1Bh} \tag{4}$$

where P is the load; C is the compliance of the DCB specimen; A_1 is the slope of the curve in the graph where a/h is plotted against $C^{1/3}$.

All experimental fatigue delamination data were interpreted via different Paris-type relations to have thorough discussions on mode I fatigue delamination behavior with fibre bridging at different R-ratios with hygrothermal aging. Particularly, the basic Paris relation Eq.(5) was used to explore fibre bridging effects on FDG behavior with hygrothermal aging. In this specific formulation, fatigue crack growth rate da/dN is linked to the fracture mechanics concept *SERR* range $\Delta\sqrt{G}$.

$$\frac{da}{dN} = C\Delta\sqrt{G}^n = C\left[\left(\sqrt{G_{max}} - \sqrt{G_{min}}\right)^2\right]^n \tag{5}$$

According to energy dissipation analysis as well as damage mechanism investigations [40], a modified Paris relation Eq.(6) has been proposed to interpret FDG behavior excluding fibre bridging, i.e. the intrinsic fatigue delamination resistance around the crack front. There is

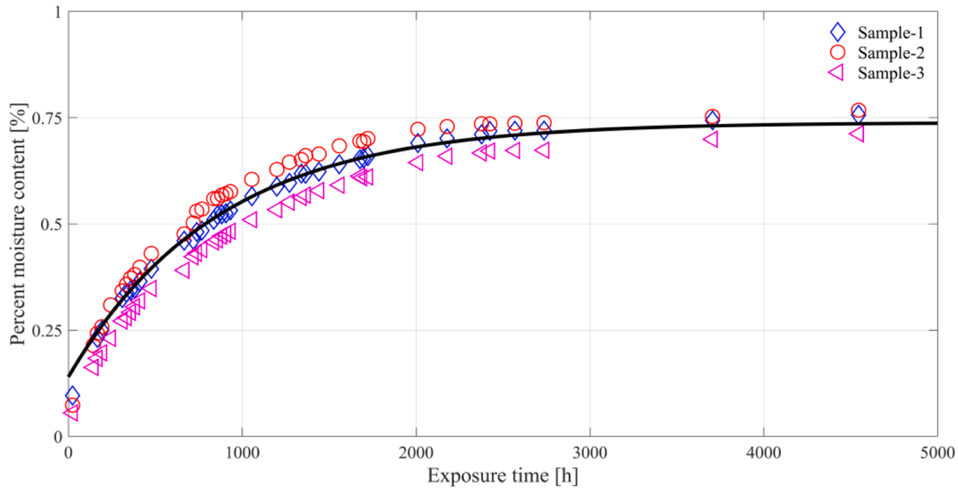

Fig. 2. Moisture absorption versus time for composite laminates M30SC/DT120.

sufficient evidence [40,41] that the use of this formulation can appropriately determine fatigue delamination behavior at a given R-ratio, which agrees well with the requirements of similitude principles.

$$\frac{da}{dN} = C\Delta\sqrt{G}^{n}_{tip} = C\left[\frac{G_{IC0}}{G_{IC}(a-a_0)}\Delta\sqrt{G}\right]^{n} \tag{6}$$

where $\Delta\sqrt{G_{\text{tip}}}$ is the *SERR* range around delamination front; $G_{\text{IC}}(a\text{-}a_0)$ represents fatigue resistance increase because of fibre bridging; and G_{IC0} is fatigue resistance excluding fibre bridging contribution.

Obvious R-ratio effects can be observed using Eq.(6) in fatigue data interpretations [41]. Thus, a new fatigue model Eq.(7), employing both $\Delta\sqrt{G_{\text{tip}}}$ and $G_{\text{max\_tip}}$ to fully describe the fatigue loading, has been recently developed to characterize FDG behavior [42]. There is evidence [41,42] that the use of this new formulation can appropriately account for R-ratio effects in FDG interpretations.

$$\frac{da}{dN} = C\Delta\sqrt{G}^{n}_{eff} = C\left[\Delta\sqrt{G}_{tip}^{\left[1-\left(\frac{G_{max\_tip}}{G_{IC0}}\right)^{\gamma}\right]} G_{max\_tip}^{\left(\frac{G_{max\_tip}}{G_{IC0}}\right)^{\gamma}}\right]^{n} \tag{7}$$

where $G_{\text{max\_tip}}$ represents the maximum *SERR* around delamination front, which can be conveniently determined via $\Delta\sqrt{G_{\text{tip}}}$ and R-ratio; and γ can be best interpreted as the weight-parameter.

3.3. DMTA experiments

DMTA experiments were conducted to have necessary information of environmental aging effects on the glass transition temperature T_g, storage modulus E' and damping factor tanδ of the composite material M30SC/DT120 used in the present study. These experiments were performed in PerkinElmer DMA8000 dynamic mechanical analyzer via single cantilever beams with dimensions of 20 mm length by 5.0 mm width and 5.0 mm thickness. All these experiments were conducted at a temperature range between 25 °C and 200 °C with a frequency of 1.0 Hz and temperature ramp rate of 5 °C/min.

4. Results and discussions

4.1. Moisture absorption analysis

Fig. 2 summarizes moisture absorption data obtained from the conditioned DCB specimens in terms of percent moisture content against immersion time. It is clear that the moisture content can significantly increase at the initial stage, and gradually flat off with long-time aging, corresponding to moisture equilibrium. The saturation moisture content was calculated as (0.75 ± 0.02)%. And these moisture uptake data were subsequently described by the Fickian diffusion law Eq.(3). The results clearly demonstrate that the use of this model can well represent moisture absorption change during the entire exposure period.

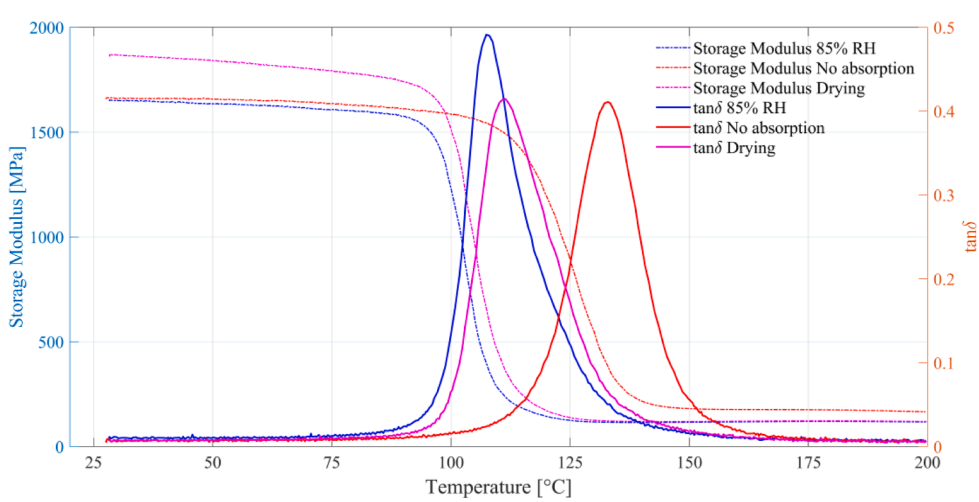

Fig. 3. Storage modulus and damping factor curves for composite laminates with/without environmental conditioning and after moisture desorption.

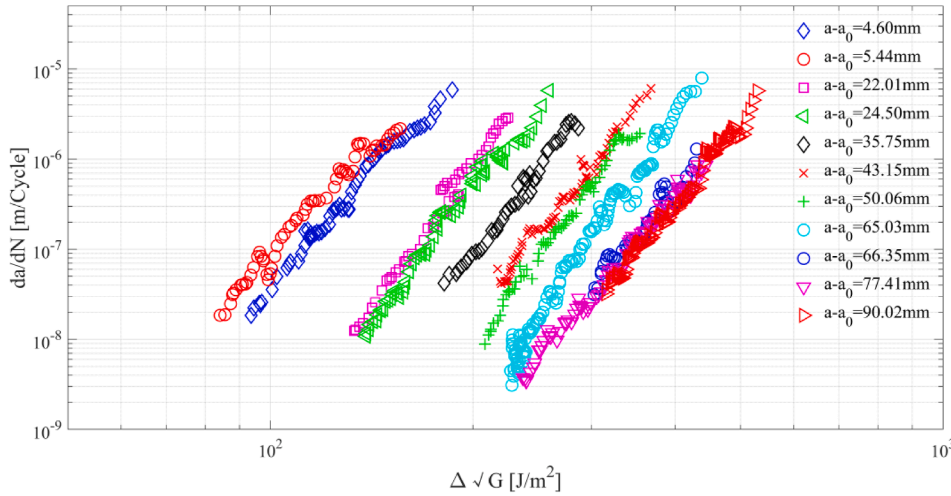

(a)

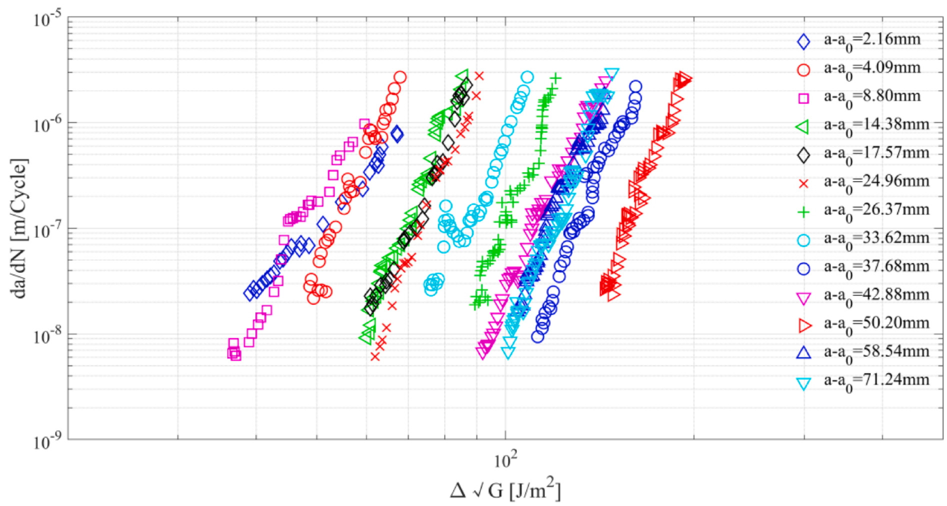

(b)

Fig. 4. Paris representation of FDG behavior with fibre bridging (a) $R = 0.1$; (b) $R = 0.5$.

4.2. DMTA results

DMTA characterizations were carried out to provide relevant information on the degree of damage/degradation in resin matrix as well as around fiber/matrix interface after hydrothermal aging. The experimental data obtained from these tests were organized in terms of storage modulus E', damping factor tanδ against temperature T, as shown in Fig. 3. Accordingly, the glass transition temperature T_g for the composite material with/without pre-conditioning, as well as after water desorption, can be conveniently determined via the peak of these tanδ curves.

There is an obvious decrease in T_g for composite material after moisture absorption (from 132.95 °C to 107.4 °C), as shown in Fig. 3. After oven drying treatment, a slight T_g recovery (i.e. 111.45 °C vs. 107.4 °C) is observed in this graph. A similar trend was also observed in the transition temperature (representing the change of material behavior from glassy state to glass-rubber transition state) in the storage modulus curves. Generally, moisture absorption in composite materials can not only lead to irreversible damage/debonding at fibre/matrix interface region or micro cracks/voids around resin matrix, but also cause reversible matrix swelling/degradation [43–45]. All these changes can finally contribute to T_g decrease of a composite material after environmental conditioning, as demonstrated in Fig. 3. It has been reported [43] that this T_g decrease, related to reversible matrix swelling/degradation, can be almost fully recovered after moisture desorption. However, in the present study, only a slight recovery of T_g is observed after water desorption as illustrated in Fig. 3. This means that there is significant irreversible damage/degradation occurrence during the aging procedure of the composite material M30SC/DT120. Detailed information related to these irreversible changes in composite will be evidenced via SEM examinations on both material microstructures and fatigue fracture surfaces in the subsequent section.

4.3. Fatigue delamination behavior interpretations

All mode I fatigue delamination data were respectively interpreted via three different Paris-type relations introduced in section 3.2 to have full understanding on FDG behavior in composite laminates after environmental aging. Particularly, the basic Paris relation Eq.(5) was used to explore fibre bridging effects on FDG behavior. The modified Paris relation Eq.(6) was employed to determine the intrinsic delamination

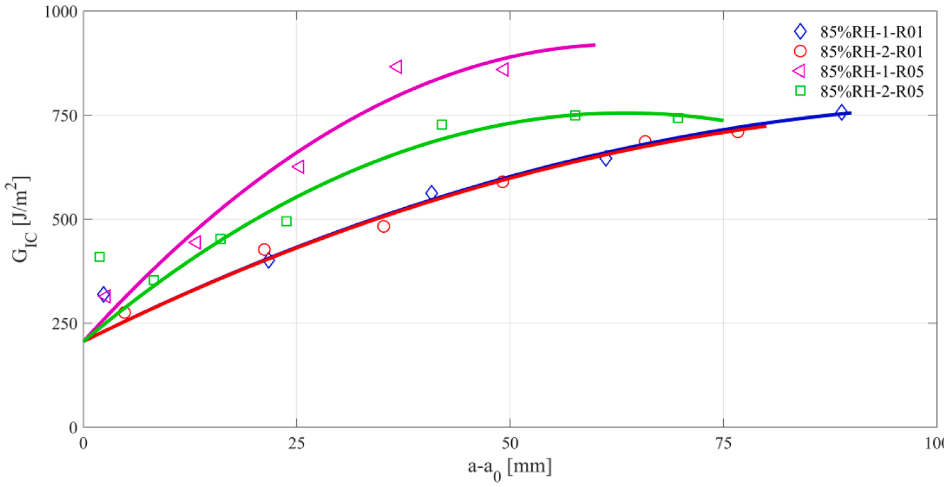

Fig. 5. Fatigue resistance curves for delamination at different *R*-ratios.

resistance around the crack front. And all these data were finally interpreted via the two-parameter Paris-type correlation Eq.(7) to account for the *R*-ratio effects in FDG interpretations, and to determine the hygrothermal aging effects on FDG behavior.

4.3.1. Paris interpretations

Fig. 4 summarizes all fatigue data at different *R*-ratios in terms of *da/dN* against $\Delta\sqrt{G}$. Significant bridging retardation effects on mode I FDG behavior were identified according to these interpretations. Particularly, the obtained Paris resistance curves can downwards shift with crack propagation (i.e. fibre bridging development), and finally collapse into a narrow band region (i.e. indicating bridging saturation). This means that the magnitude of *da/dN* at a given $\Delta\sqrt{G}$ is not constant, but decreases significantly with crack propagation for fibre-bridged FDG. As discussed in the previous studies [40,46], the presence of bridging fibres in the wake of delamination front is the main reason for this retardation. Particularly, more bridging fibres can be present in a longer crack growth, contributing to more strain energy being cyclically stored and released in them under fatigue loading. And there is a saturation of fibre bridging development, in which the new generation of bridging fibres around the crack front can balance with the final failure of bridging fibres at the end of bridging region. As a result, the Paris resistance curves with really long crack propagation intend to converge into a narrow band region, as shown in Fig. 4.

The results illustrated in Fig. 4 clearly demonstrate that the presence of fibre bridging can cause mode I FDG behavior crack length dependence, once using the Paris relation in fatigue data interpretations. This indeed violates the basic requirements of the similitude principles. In accordance with this hypothesis, FDG behavior in the same composite at the same *SERR* should be the same or at least similar, regardless of crack propagation length [47,48]. As a result, a new similitude parameter, appropriately representing the similarity in FDG, should be proposed and applied to determine FDG behavior with fibre bridging. The modified Paris relation [40], employing the *SERR* range $\Delta\sqrt{G_{tip}}$ applied around delamination front, will be subsequently used to interpret fibre-bridged FDG behavior.

4.3.2. Modified Paris interpretations

As a prerequisite of using Eq.(6) in fatigue data interpretations, fatigue *R*-curves $G_{IC}(a\text{-}a_0)$ must be determined in advance in order to calculate the *SERR* range $\Delta\sqrt{G_{tip}}$ around the crack front. And it should be stressed that the magnitude of fatigue *R*-curve differs from that in quasi-static delamination, physically making it incorrect to directly use quasi-static *R*-curve in fatigue data analysis [46]. Thus, the fatigue *R*-curve for each tested DCB specimen was carefully determined via the specific test procedure introduced in the section 3.1, in order to use this modified Paris relation in fibre-bridged FDG interpretations.

Fig. 5 summarizes all fatigue *R*-curves in terms of interlaminar resistance G_{IC} against crack propagation length $a\text{-}a_0$. It is clear that there is significant increase in G_{IC} with delamination growth because of fibre bridging for both *R*-ratios. No obvious scatter was observed for $R = 0.1$. However, some scatter was identified for $R = 0.5$, which may be related to the deviations in fibre bridging generation during FDG. Furthermore, the magnitude of $G_{IC}(a\text{-}a_0)$ for $R = 0.5$ is slightly higher than that of $R =$

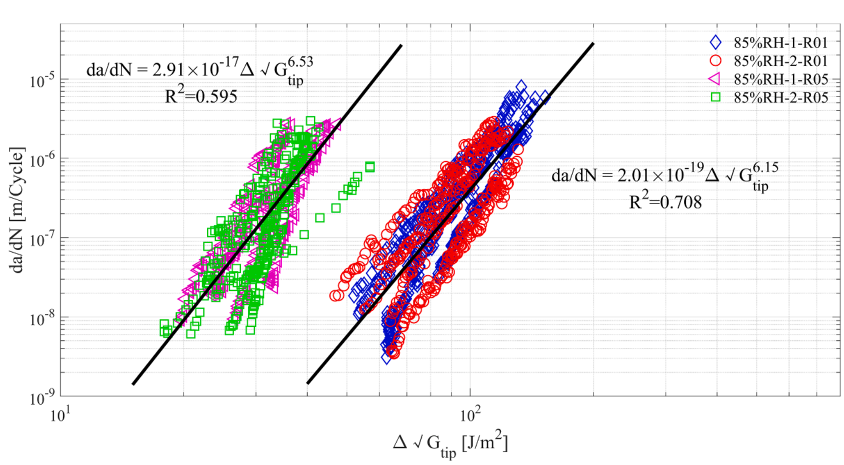

Fig. 6. Fatigue data interpretations via the modified Paris relation.

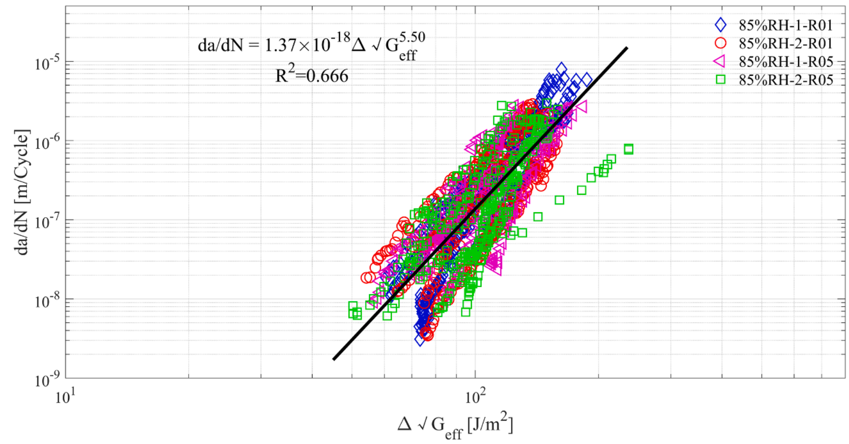

Fig. 7. Fatigue data interpreted via the two-parameter Paris-type relation.

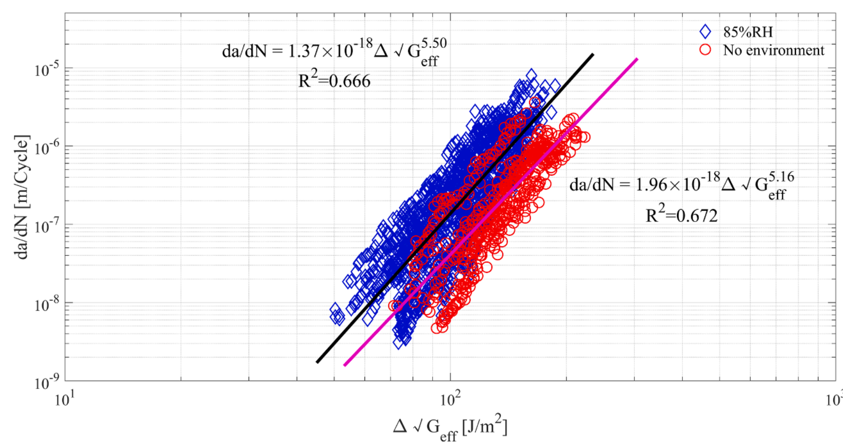

Fig. 8. Hygrothermal aging effects on fatigue delamination behavior.

0.1, indicating more fibre bridging generation in fatigue delamination at a higher *R*-ratio. The possible reason (i.e. crack closure) for this difference has been given in the previous studies [49,50]. Particularly, the resistance increase for each tested specimen can be well fitted via a second-order polynomial function as demonstrated in Fig. 5.

According to these fitted resistance curves, mode I fatigue data of each tested specimen can be interpreted via the modified Paris relation Eq.(6). All these interpretations are summarized in terms of *da/dN* against $\Delta\sqrt{G_{tip}}$, as illustrated in Fig. 6. It is clear that fatigue data with different crack propagation can converge into a narrow band region, as compared to the interpretations illustrated in Fig. 4. This means FDG behavior for the same *SERR* remains the same or at least similar, which obeys well with the similitude principles. And there is good repeatability for fatigue experiments at the same *R*-ratio. As a result, a master resistance curve can be fitted to appropriately represent FDG behavior. Furthermore, there is still obvious *R*-ratio dependence using this correlation in fibre-bridged FDG interpretations. Particularly, FDG rate of $R = 0.5$ is much faster than that of $R = 0.1$ at a given $\Delta\sqrt{G_{tip}}$.

It has been reported [40] that most permanent energy dissipation in fibre-bridged FDG indeed concentrates around the crack front, and fibre bridging indeed has negligible contribution to permanent energy release. This is the physical reason for the validity of using Eq.(6) with $\Delta\sqrt{G_{tip}}$ as the similitude parameter in fibre-bridged mode I FDG characterization. Particularly, the use of this formulation in fibre-bridged fatigue interpretations indeed represents damage propagation around the crack front, i.e. the intrinsic delamination resistance. Thus, the results illustrated in Fig. 6 demonstrate that the intrinsic delamination resistance remains the same or similar for fatigue delamination with fibre bridging at a given *R*-ratio, i.e. there is no crack length dependence in FDG.

4.3.3. Two-parameter model interpretations

All fatigue data of different *R*-ratios were finally interpreted via Eq.(7) to account for *R*-ratio effects. Different from Eq.(6), both $\Delta\sqrt{G_{tip}}$ and G_{max_tip} were employed in FDG interpretations in the perspective of fully describing fatigue loading. It is clear that the use of this correlation can well account for *R*-ratio effects, as illustrated in Fig. 7. Particularly, all fatigue data of different *R*-ratios can collapse into a narrow band region, contributing to a master resistance curve in representing mode I FDG behavior at various *R*-ratios.

In our previous studies [40,49,51], mode I fatigue delamination experiments have been carried out at two different *R*-ratios (i.e. $R = 0.1$ and 0.5) with different amounts of fibre bridging without hygrothermal aging. The use of Eq.(7) in fatigue data interpretations makes the possibility of exploring hygrothermal aging effects on FDG behavior at different stress ratios. All these results are summarized and compared in terms of *da/dN* against $\Delta\sqrt{G_{eff}}$, as shown in Fig. 8. And a master resistance curve can be respectively fitted to represent FDG behavior in composite laminates with or without hygrothermal aging. It is clear that hygrothermal aging has significantly detrimental effects on the intrinsic FDG behavior. Particularly, FDG in composite with water absorption is much faster than that without moisture absorption. In general, as discussed in the literature [43–46], moisture immersion induced degradation in matrix and around fibre/matrix interface may be the reason for this FDG acceleration. And detailed evidence to explain this FDG increase will be provided and discussed via the SEM observations on both

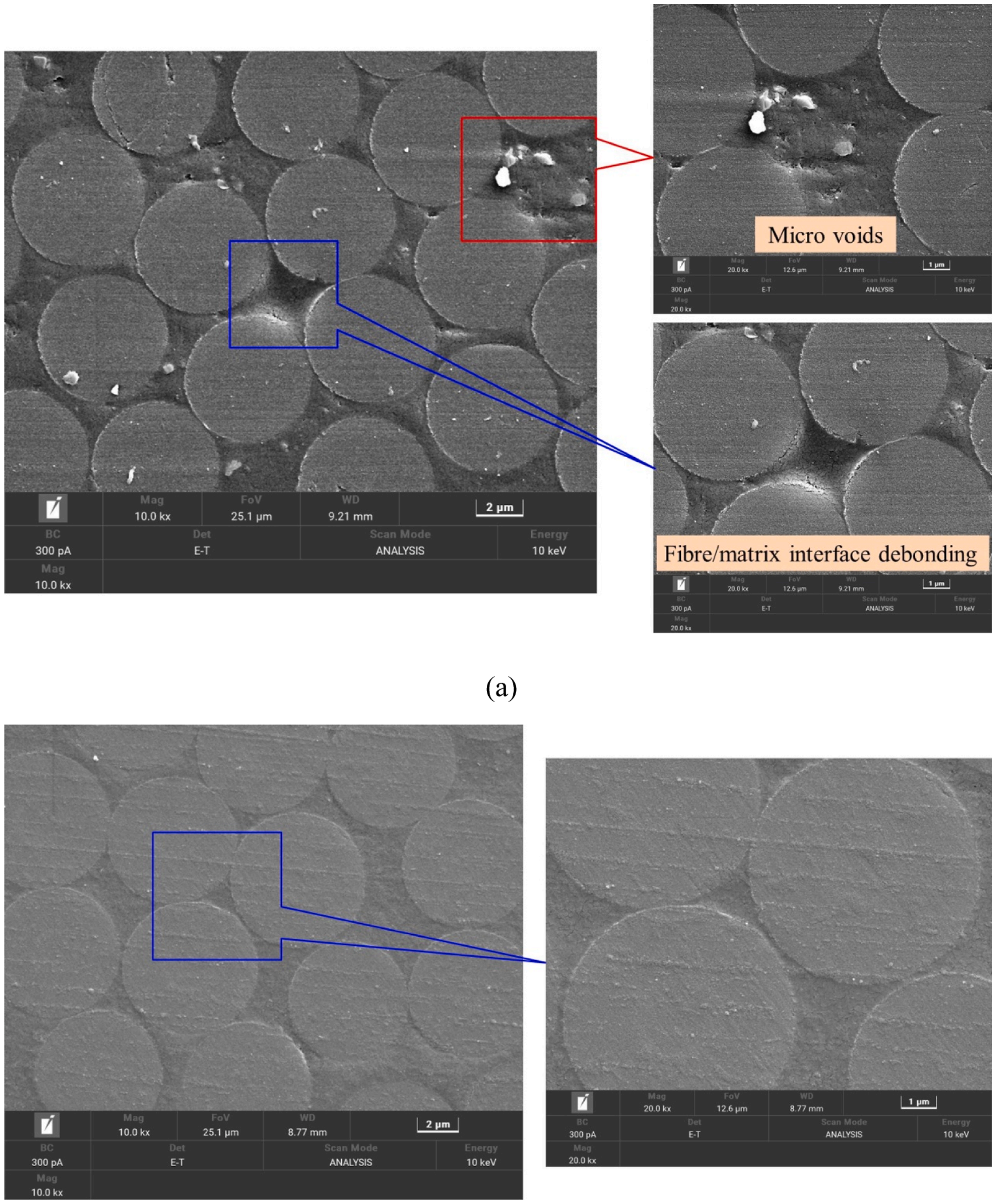

Fig. 9. Morphology of composite laminates with/without hygrothermal conditioning (a) Environmental aged composite; (b) No environmental aged composite.

material morphology and fatigue fracture surfaces.

5. Damage mechanisms in FDG of composite laminates with environmental conditioning

SEM examinations were first conducted on composite with/without water uptake, to have detailed information on hygrothermal aging effects on material morphology. Fractographic SEM observations were subsequently performed on fatigue fracture surfaces of different *R*-ratios, to explore the damage mechanisms in delamination growth as well as to provide the physical reasons for the results that illustrated in Fig. 8.

5.1. Fractographic analysis on material microstructure

Fig. 9 provides morphology of composite with/without environmental aging. Some important differences can be clearly identified in the composite after hygrothermal conditioning, as compared to that without moisture absorption. Particularly, both fibre/matrix interface debonding and micro voids induced by water absorption were clearly observed in composite material with hygrothermal aging, as illustrated in Fig. 9 (a). However, these micro features are not obvious in composite without environmental aging. Particularly, the material remains intact as shown in Fig. 9(b). Referring to the previous discussions on T_g decrease in environmental aged composite, these observations can provide necessary evidence to physically interpret the T_g decrease that illustrated in Fig. 3. In addition, it should be noted that resin matrix property

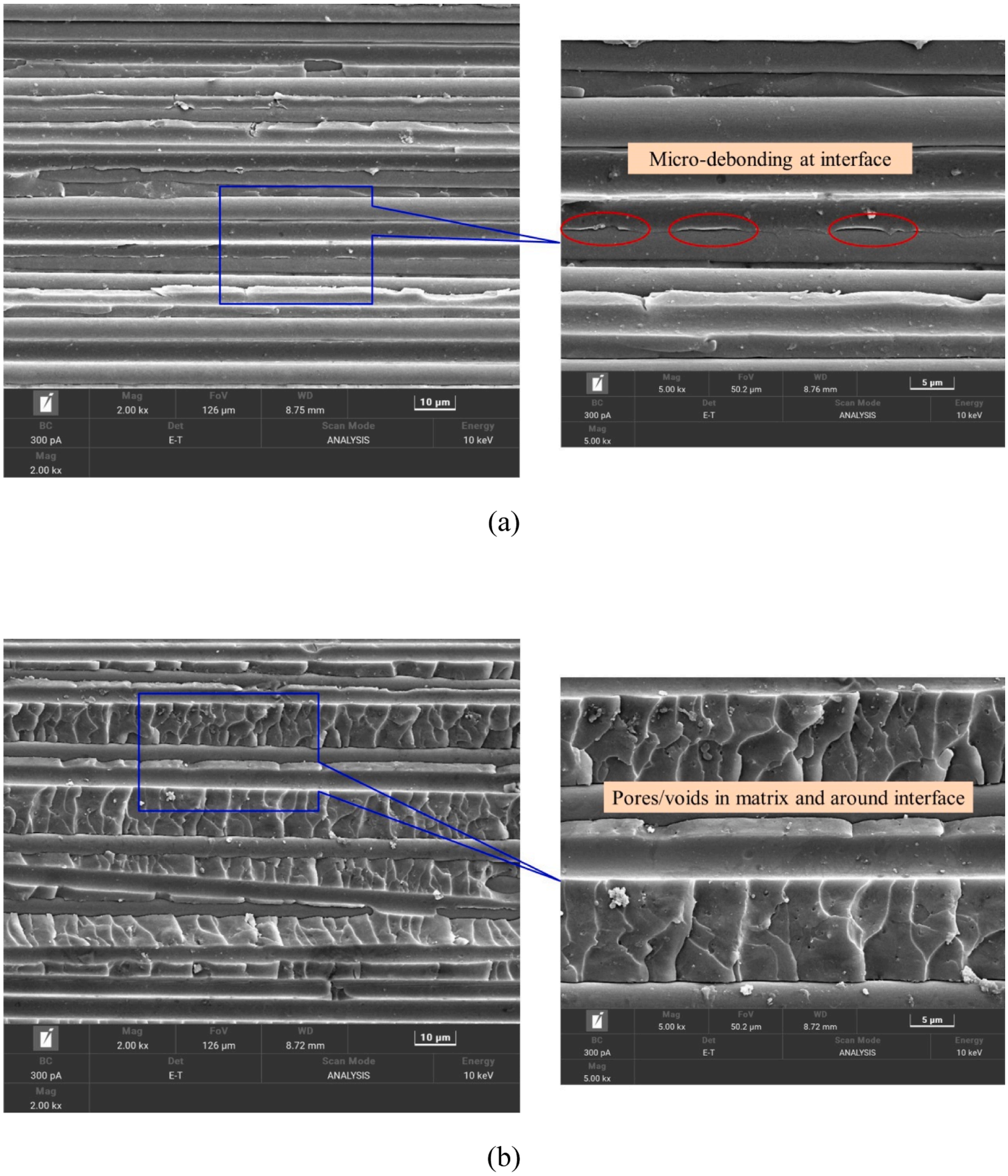

Fig. 10. SEM observations on fatigue fracture surfaces of $R = 0.1$ (a) Dominant fibre/matrix debonding; (b) Matrix brittle failure at local region.

degradation (such as plasticization) induced by water uptake can be partly or fully recovered after water desorption. However, this observed irreversible damage, i.e. interface debonding and matrix pores, cannot be recovered after drying. As a result, only a slight increase of T_g for conditioned composite with drying treatment is observed as shown in Fig. 3.

5.2. Fractographic examinations on fatigue fracture surfaces

Figs. 10 and 11 summarize SEM observations on mode I fatigue fracture surfaces of composite laminates at different R-ratios after environmental conditioning. Both fibre print and matrix brittle fracture failure were identified on the delamination surfaces for both R-ratios. Particularly, fibre print, resulting from fibre/matrix interface debonding, is the dominant microscopic feature distributed on mode I delamination surface. Matrix brittle fracture, characterized by riverlines, scarps and hackles, was also identified at some locations on the delamination surface. And no obvious matrix plastic deformation was found on the delamination surface. In addition to above mentioned microscopic features (which has also been reported in fatigue delamination without environmental conditioning [40]), some new microscopic features were found on these delamination surfaces with hygrothermal aging. The first important new feature is micro-debonding at fibre/matrix interface, as indicated in the red circle in Figs. 10(a) and 11(a). The second important new feature is obvious micro-void that distributed in matrix and around fibre/matrix interface, as illustrated in Figs. 10(b) and 11(b). These micro features were not reported in fatigue delamination of the same composite without environmental conditioning [40]. To the authors' opinion, the presence of these additional features is closely related to hygrothermal aging. Particularly, water uptake around fibre/matrix interface region due to the capillary effects can weaken interface adhesion and finally lead to this micro-debonding feature, as illustrated in Figs. 10(a) and 11(a). And long-term moisture absorption in the resin matrix can not only gradually result in micro-void generation in the matrix material, but also tend to promote above mentioned micro-debonding at the interface region, as shown in Figs. 10 and 11.

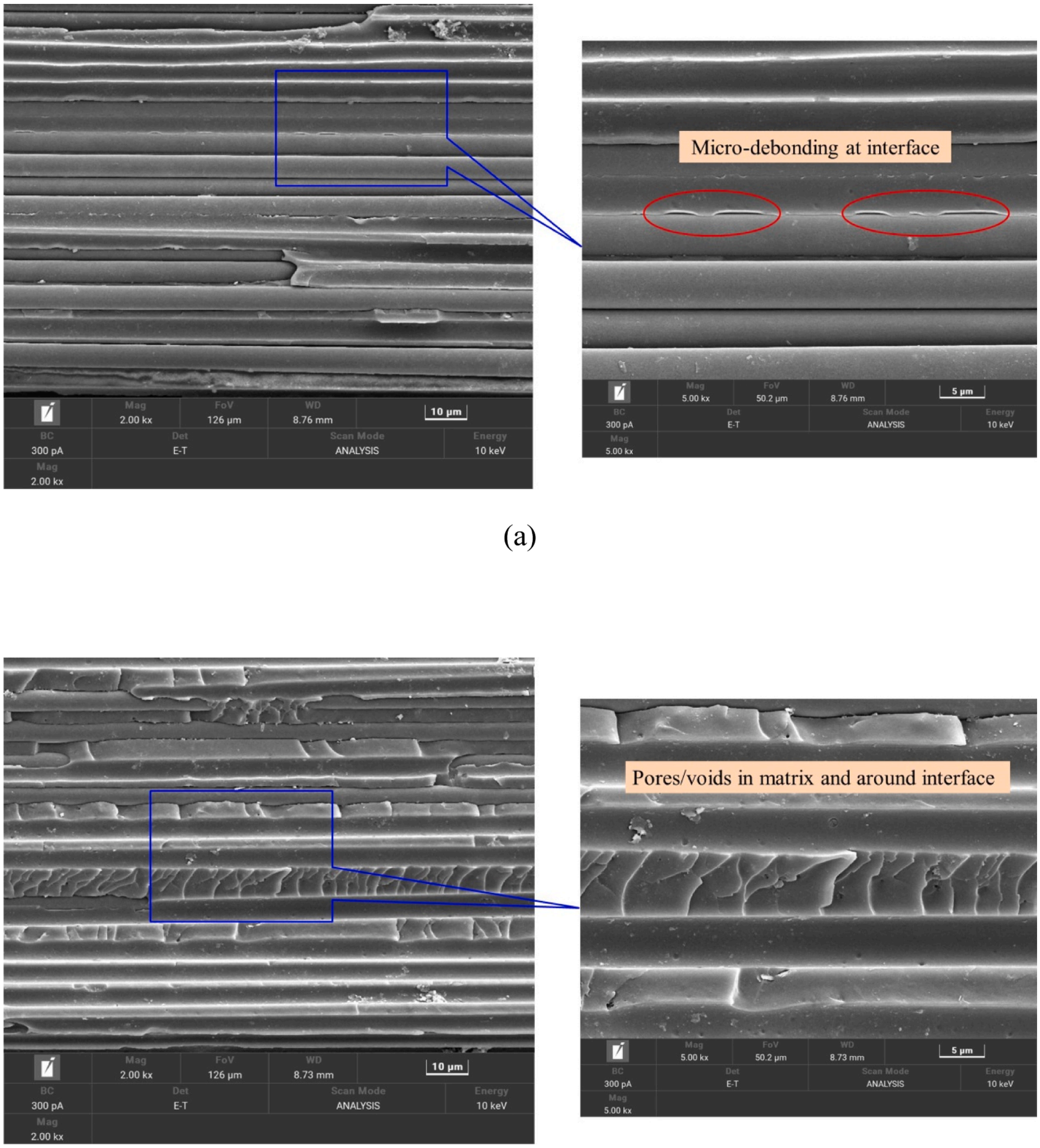

(b)

Fig. 11. SEM observations on fatigue fracture surfaces of $R = 0.5$ (a) Dominant fibre/matrix debonding; (b) Matrix brittle failure at local region.

As discussed above, the dominant damage mechanisms in mode I fatigue delamination for composite laminates with environmental conditioning remain the same to that without hygrothermal aging. Both fibre prints and matrix brittle fracture were identified on the fatigue delamination surfaces. However, there is evidence that hygrothermal aging can have significantly detrimental effects on matrix property (i.e. the presence of pores/voids) and fibre/matrix bonding performance (i.e. micro debonding generation). These are the physical reasons for the FDG increase as illustrated in Fig. 8, i.e. hygrothermal aging can accelerate FDG behavior. Furthermore, this adverse influence can result in some new features distributed on fatigue delamination surfaces.

6. Conclusions

Hygrothermal aging effects on mode I fatigue delamination behavior with fibre bridging in composite laminates have been thoroughly investigated in the present study. Three different Paris-type correlations were employed to explore FDG behavior. These interpretations based on the Paris relation demonstrate that fibre bridging has important retardation effects on FDG behavior. The use of the modified Paris relation can well represent the similarity in fibre-bridged FDG, contributing to a master resistance curve in determining the intrinsic FDG behavior at a given R-ratio. The use of the two-parameter Paris-type relation can appropriately account for R-ratio effects, making a master resistance curve in characterizing FDG behavior at different R-ratios. Furthermore, fatigue data interpreted via this two-parameter correlation clearly demonstrated that hygrothermal aging has detrimental effects on mode I FDG behavior of composite laminates.

Fractographic analysis demonstrated that environmental aging can have important effects on the microstructures of composite laminates. Particularly, both pores/voids in resin matrix and debonding at fibre/matrix interface were identified in composite because of environmental conditioning. However, no obvious difference in damage mechanisms was identified in mode I FDG for composite with/without water immersion. Both dominant fibre prints and local matrix brittle fracture were observed on the delamination surfaces. And no matrix plastic deformation was found in fatigue delamination with environmental aging. Accordingly, it can be concluded that the major reason for hygrothermal aging detrimental effects on mode I FDG behavior is related to the degradation of interface adhesion and resin matrix that induced by water absorption.

CRediT authorship contribution statement

Liaojun Yao: Conceptualization, Data curation, Formal analysis, Funding acquisition, Investigation, Methodology, Project administration, Resources, Software, Supervision, Validation, Visualization, Writing – original draft, Writing – review & editing. **Jiexiong Wang:** Formal analysis, Software, Validation, Visualization. **Yonglyu He:** Data curation, Formal analysis, Investigation, Writing – original draft. **Xiuhui Zhao:** Formal analysis, Investigation. **Xiangming Chen:** Funding acquisition, Validation. **Jurui Liu:** Methodology, Software, Validation. **Licheng Guo:** Data curation, Formal analysis. **R.C. Alderliesten:** Data curation, Methodology, Supervision.

Declaration of competing interest

The authors declare that they have no known competing financial interests or personal relationships that could have appeared to influence the work reported in this paper.

Data availability

Data will be made available on request.

Acknowledgement

The authors gratefully acknowledge financial support from the National Natural Science Foundation of China with Grant No. 12272110, 11902098 and 12272358, the Aeronautical Science Foundation of China with Grant No. 2022Z055077004, the National Key Laboratory of Strength and Structural Integrity Foundation with Grant No. ASSIKFJJ202302003.

References

[1] Khan, R. Delamination growth in composites under fatigue loading. Ph. d Dissertation of TU Delft, 2013.
[2] Bak BLV, Sarrado C, Turon A, Costa J. Delamination under fatigue loads in composite laminates: A review on the observed phenomenology and computational methods. Appl Mech Rev 2014;66:060803.
[3] Blondeau C, Pappas GA, Botsis J. Crack propagation in CFRP laminates under mode I monotonic and fatigue loads: A methodology study. Compos Struct 2021;256: 113002.
[4] Amaral L, Alderliesten R, Benedictus R. Understanding mixed-mode cyclic fatigue delamination growth in unidirectional composites: An experimental approach. Eng Fract Mech 2017;180:161–78.
[5] Federal Aviation Authority. Airworthiness advisor circular No: 20-107B. Composite Aircraft Structure 2009.
[6] Stelzer S, Brunner AJ, Arguelles A, Murphy N, Pinter G. Mode I delamination fatigue crack growth in unidirectional fiber reinforced composites: Development of a standardized test procedure. Compos Sci Technol 2012;72:1102–7.
[7] Murri GB. Effect of data reduction and fiber-bridging on mode I delamination characterization of unidirectional composites. J Compos Mater 2014;48:2413–24.
[8] Stelzer S, Brunner AJ, Arguelles A, Murphy N, Cano GM, Pinter G. Mode I delamination fatigue crack growth in unidirectional fiber reinforced composites: Results from ESIS TC4 round-robins. Eng Fract Mech 2014;116:92–107.
[9] Pascoe JA, Alderliesten RC, Benedictus R. Methods for the prediction of fatigue delamination growth in composites and adhesive bonds- A critical review. Eng Fract Mech 2013;112-113:72–96.
[10] Blanco N, Gamstedt EK, Asp LE, Costa J. Mixed-mode delamination growth in carbon-fibre composite laminates under cyclic loading. Int J Solids Struct 2004;41: 4219–35.
[11] Hojo M, Ando T, Tanaka M, et al. Mode I and Mode II interlaminar fracture toughness and fatigue delamination of CF/epoxy laminates with self-same epoxy interleaf. Int J Fatigue 2006;28:1154–65.
[12] Zhao L, Gong Y, Zhang J, Wang Y, Lu Z, Peng L, et al. A novel interpretation of fatigue delamination growth behavior in CFRP multidirectional laminates. Compos Sci Technol 2016;133:79–88.
[13] Murri, G.B. Evaluation of delamination onset and growth characterization methods under mode I fatigue loading. NASA/TM-2013-217966.
[14] O'Brien, T.K, Johnston, W.M, Toland, G.J. Mode II interlaminar fracture toughness and fatigue characterization of a graphite epoxy composite material. NASA/TM-2010-216838.
[15] Simon I, Bank-Sills L, Fourman V. Mode I delamination propagation and R-ratio effects in woven composite DCB specimens for a multi-directional layup. Int J Fatigue 2017;96:237–51.
[16] Fulco APP, de Medeiros AM, Tonatto MLP, et al. Fatigue damage and fatigue life diagrams of a carbon/epoxy cross ply laminate aged by hygrothermal exposure. Compos A Appl Sci Manuf 2019;127:105628.
[17] Behera A, Dupare P, Thawre MM, Ballal A. Effects of hygrothermal aging and fiber orientations on constant amplitude fatigue properties of CFRP multidirectional composite laminates. Int J Fatigue 2020;136:105590.
[18] Alam P, Robert C, Bradaigh CMO. Tidal turbine blade composites- A review on the effects of hygrothermal aging on the properties of CFRP. Compos B Eng 2018;149: 248–59.
[19] Aceti P, Carminati L, Bettini P, Sala G. Hygrothermal ageing of composite structures. Part 1: Technical review. Compos Struct 2023;319:117076.
[20] Alessi S, Pitarresi G, Spadaro G. Effect of hydrothermal ageing on the thermal and delamination fracture behaviour of CFRP composites. Compos B Eng 2014;67: 145–53.
[21] Xian G, Li H, Su X. Effects of immersion and sustained bending on water absorption and thermomechanical properties of ultraviolet cured glass fiber-reinforced acylate polymer composites. J Compos Mater 2012;47:2275–85.
[22] Tserpes K, Tzatzadakis V, Katsiropoulos C. Effect of hygrothermal ageing on the interlaminar shear strength of carbon fiber-reinforced rosin-based epoxy bio-composites. Compos Struct 2019;226:111211.
[23] Kafodya I, Xian G, Li H. Durability study of pultruded CFRP plates immersed in water and seawater under sustained bending: Water uptake and effects on the mechanical properties. Compos B Eng 2015;70:138–48.
[24] Davidson BD, Kumar M, Soffa MA. Influence of mode ratio and hygrothermal condition on the delamination toughness of a thermoplastic particulate interlayered carbon/epoxy composite. Compos A Appl Sci Manuf 2009;40:67–79.
[25] Toscano A, Pitarresi G, Scafidi M, et al. Water diffusion and swelling stresses in highly crosslinked epoxy matrices. Polym Degrad Stab 2016;133:255–63.
[26] Meng M, Rizvi MJ, Grove SM, Le HR. Effects of hygrothermal stress on the failure of CFRP composites. Compos Struct 2015;133:1024–35.
[27] Tsenoglu CJ, Pavlidou S, Papaspyrides CD. Evaluation of interfacial relaxation due to water absorption in fiber-polymer composites. Compos Sci Technol 2006;66: 2855–64.
[28] Costa ML, De Almeida SFM, Rezende MC. Hygrothermal effects on dynamic mechanical analysis and fracture behavior of polymeric composites. Mater Res 2005;8:335–40.
[29] Ray BC. Temperature effect during humid ageing on interfaces of glass and carbon fibers reinforced epoxy composites. J Colloid Interface Sci 2006;298:111–7.
[30] Gu Y, Liu H, Li M, Li Y, Zhang Z. Macro- and micro-interfacial properties of carbon fiber reinforced epoxy resin composite under hygrothermal treatments. J Reinf Plast Compos 2014;33(4):369–79.
[31] Asp LE. The effects of moisture and temperature on the interlaminar delamination toughness of a carbon/epoxy composite. Compos Sci Technol 1998;58:967–77.
[32] Mamalis D, Floreani C, Bradaigh CMO. Influence of hygrothermal ageing on the mechanical properties of unidirectional carbon fibre reinforced powder epoxy composites. Compos B Eng 2021;225:109281.
[33] Sales RCM, de Sousa AF, Brito CBG, et al. Analysis of hygrothermal effects on mixed mode I/II interlaminar fracture toughness of carbon composite joints. Int J Adhes Adhes 2020;97:102477.
[34] Nakai Y, Hiwa C. Effects of loading frequency and environment on delamination fatigue crack growth of CFRP. Int J Fatigue 2002;24:161–70.
[35] LaPlante G, Landry B. The effect of hygrothermal aging on mode I fatigue delamination growth in a carbon/epoxy composite. J Adv Mater 2011;43:79–86.
[36] Landry B, LaPlante G, LeBlanc LR. Environmental effects on mode II fatigue delamination growth in an aerospace grade carbon/epoxy composite. Compos A Appl Sci Manuf 2012;43:475–85.
[37] Ramirez FMG, Garpelli FP, et al. Hygrothermal effects on the fatigue delamination growth onset in interlayer toughened CFRP joints. Int J Fatigue 2020;138:105729.
[38] van den Akker BPH, Donadon MV, Loendersloot R, et al. The influence of hygrothermal ageing on the fatigue behavior and residual strength of post-buckled co-bonded stiffened panels subjected to compression loading. Compos B Eng 2020; 194:108023.
[39] ASTM D5229. Standard test method for moisture absorption properties and equilibrium conditioning of polymer matrix composite materials.
[40] Yao L, Sun Y, Guo L, Zhao M, Jia L, Alderliesten RC, et al. A modified Paris relation for fatigue delamination with fibre bridging in composite laminates. Compos Struct 2017;176:556–64.
[41] Yao L, Chuai M, Liu J, Guo L, Chen X, Alderliesten RC, et al. Fatigue delamination behavior in composite laminates at different stress ratios and temperatures. Int J Fatigue 2023;175:107830.
[42] Yao L, Cui H, Guo L, Sun Y. A novel total fatigue life model for delamination growth in composite laminates under generic loading. Compos Struct 2021;258: 113402.
[43] Wang Z, Xian G, Zhao XL. Effects of hydrothermal aging on carbon fibre/epoxy composites with different interfacial bonding strength. Constr Build Mater 2018; 161:634–48.

[44] Khan LA, Mahmood AH, Syed AS, Khan ZM, Day RJ. Effect of hygrothermal conditioning on the fracture toughness of carbon/epoxy composites cured in autoclave/Quickstep. J Reinf Plast Compos 2013;32:1165–76.
[45] Fang W, Guo W. Deterioration mechanism of hydrothermal aging on the properties of carbon fiber/epoxy composites in various media. J Compos Mater 2023;57:1235–46.
[46] Yao L, Alderliesten R, Zhao M, Benedictus R. Bridging effect on mode I fatigue delamination behavior in composite laminates. Compos A Appl Sci Manuf 2014;63:103–9.
[47] Jones R, Kinloch AJ, Hu W. Cyclic-fatigue crack growth in composite and adhesively-bonded structures: The FAA slow crack growth approach to certification and the problem of similitude. Int J Fatigue 2016;88:10–8.
[48] Cano AJ, Salazar A, Rodriguez J. Evaluation of different crack driving forces for describing the fatigue crack growth behavior of PET-G. Int J Fatigue 2018;107:27–32.
[49] Yao L, Sun Y, Zhao M, Alderliesten RC, Benedictus R. Stress ratio dependence of fibre bridging significance in mode I fatigue delamination growth of composite laminates. Compos A Appl Sci Manuf 2017;95:65–74.
[50] Khan R, Alderliesten R, Yao L, Benedictus R. Crack closure and fibre bridging during delamination growth in carbon fibre/epoxy laminates under mode I fatigue loading. Compos A Appl Sci Manuf 2014;67:201–11.
[51] Yao L, Alderliesten RC, Benedictus R. The effect of fibre bridging on the Paris relation for mode I fatigue delamination growth in composites. Compos Struct 2016;140:125–35.